DESIGN AND MODELING OF HIGH SPEED PIN PHOTODETECTOR FOR 50 GB/S OPTICAL FIBER LINKS

BY

YU-TING PENG

THESIS

Submitted in partial fulfillment of the requirements
for the degree of Master of Science in Electrical and Computer Engineering
in the Graduate College of the
University of Illinois at Urbana-Champaign, 2017

Urbana, Illinois

Adviser:

Professor Milton Feng

ABSTRACT

High speed optical interconnect holds the key to the future Internet revolution; optical fibers have replaced traditional copper wires over long distances within data centers and high performance computing (HPC) due to their speed and reliability. With the increasing demand for high speed data transmission in data center and cloud computing applications, the development of optical transceivers has become indispensable. To complement high speed transmitters in optical links, high speed receiver devices, known as photodetectors, need to be designed properly so as not to present a bottleneck in the performance of optical links. With the aid of microwave modeling, we can characterize the performance of the photodetector and therefore improve the devices. This work will present the quantitative design and analysis of the P-i-N photodetector which is capable of operating at 50 Gb/s data rate for energy efficient transmission.

ACKNOWLEDGMENTS

I would like to thank Professor Milton Feng for the guidance and advice he provided not only to my research work but also to my personal life. He is such a role model for me to follow as a hardworking and intelligent engineer in the field of semiconductors. I am very grateful to have the opportunity to work on the photodetector project under his supervision. I also want to thank all the members in my group, Ardy Winoto, Cutis Wang, Junyi Qiu, Hsiao-Lun Wang, Xin Yu, Adam Auten, Dufei Wu and Wenning Fu, for the generous help throughout the work. Finally I would like to thank my family and friends for the support in my pursuit of knowledge and career.

TABLE OF CONTENTS

1. Introduction

1.1 Motivation

The increasing demand for high speed data transmission in data center and cloud computing applications promotes the development of optical interconnects. A forecast of traffic growth in data centers from Cisco shown in Fig. 1 predicts that there will be 14.1 zettabytes (10^{21} bytes) of data transmission by 2020. Optical interconnects are massively deployed to accommodate the elevated traffic growth in data centers as they provide better performance compared to traditional copper cables in high speed data transmission. Traditional electrical cables have two inherent weaknesses compared to optical interconnects. First, the parasitic capacitance and resistance in electrical cables will rise when scaling down and therefore they have longer RC time constant which causes more delay in data transmission. Second, skin effect and cross talk both introduce unfavorable noise and interference during signal transmission at high frequency. On the other hand, optical fiber does not suffer from electrical signal delay, and has higher bandwidth and less signal loss. Figure 2 shows that compared to electrical cables, optical cables have less attenuation and are free from adverse effects of high frequency, making them more favorable for use as a high speed transmission medium.

A typical fiber-based optical interconnect consists of three parts as shown in Fig. 3: an optical transmitter, fiber as the transmission medium, and an optical receiver. The transmitter comprises a laser diode driver (LDD) and vertical cavity surface emitting laser (VCSEL). The VCSEL is most widely used today especially in short reach applications due to its low power consumption (low threshold current) and high bandwidth. On the other end, the receiver is assembled from a photodetector, transimpedance amplifier (TIA) and limiting amplifier (LA). LA protects the circuits by limiting the amplitude of the input signal before it enters into the following stages. TIA acts as an element to convert current into voltage signal. In terms of the photodetector in the receiver, a P-i-N structure is the most deployed due to its easy fabrication and low noise (low dark current).

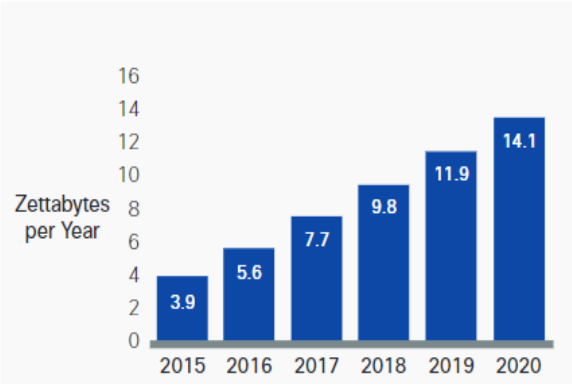

Figure 1: Cloud data center traffic growth [2]

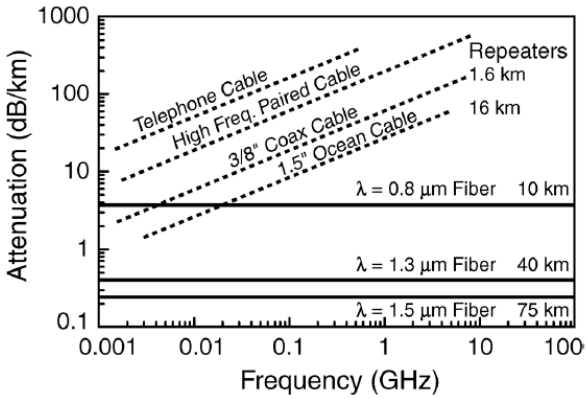

Figure 2: Electrical and optical interconnect attenuation as a function of frequency [3]

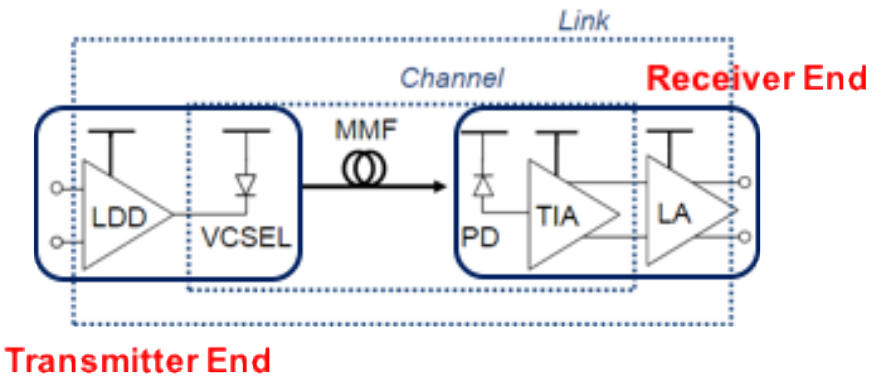

Figure 3: Transceiver links in optical interconnects at 25 Gb/s [5]

1.2 Principles of P-i-N photodetector

A schematic of a P-i-N junction with its energy band diagram is shown in Fig. 4. When light with photon energy larger than the energy gap is absorbed in the intrinsic region, electron-hole pairs are generated in the junction. For high speed operation, we want to transport the photogenerated carriers to the corresponding contacts as quickly as possible. This process is facilitated by applying a reverse bias to the junction, inducing a high electric field in the depleted intrinsic region which sweeps the carriers at the saturation drift velocity. The speed of the P-i-N photodetector is determined by two factors: transit time delay and RC charging time. Transit time corresponds to the delay that photogenerated electrons and holes need to reach the n and p contacts. Since electrons and holes are generated in pairs, we need to consider the saturation velocity of electrons and holes when characterizing the bandwidth limited by the transit time delay. Assuming there is no recombination in the intrinsic layer due to the thickness being at the same order of $\frac{1}{\alpha}$, where α is the absorption coefficient of the material, the light is absorbed inside the intrinsic region only. Furthermore, since the light is shined on the intrinsic layer as a series of pulses with time variation, we can assume a uniform generation with respect to transit time delay and the frequency limited by transit time delay for simplicity. By solving the continuity equation for both electrons and holes with the uniform generation function, substituting any terms relevant to holes in terms related to electrons with scaling constants, we can obtain the expression shown below with the definition of the worst case transit time delay equal to total intrinsic layer thickness divided by the saturation velocity of electrons:

$$f_{3dB,transit} = \frac{0.48 v_{sat,n}}{T_{intrinsic}} \text{ [1,4]}$$

Therefore, we know transit time delay is relevant to the saturation velocity of electrons, which is assumed constant with the applied field in the intrinsic layer, and the thickness of the intrinsic layer ($T_{intrinsic}$). The constant before saturation velocity comes from the half-power solution in frequency response. When the square of the magnitude of frequency response equals $\frac{1}{2}$, we can

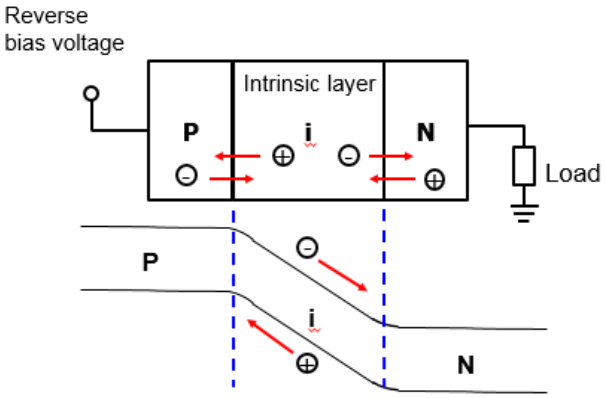

Figure 4: Schematic of a P-i-N junction

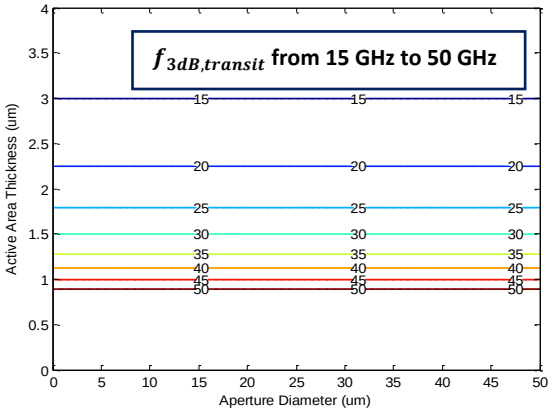

Figure 5: Transit time delay limited bandwidth vs. different aperture diameters and thickness of intrinsic layer

find a solution of $\omega\tau_{transit}$,where ω ($\omega = 2\pi f_{3dB,transit}$) is the angular frequency, and then substitute $\tau_{transit}$ as defined earlier to extract this scaling constant.

Based on the expression, the simulation of transit time delay limited bandwidth from 15 GHz to 50 GHz versus different aperture sizes and thickness of intrinsic layer is shown in Fig. 5. In order to increase the bandwidth, the thickness of the intrinsic layer needs to be decreased, which reduces the time for electrons and holes to drift through the intrinsic layer. The second factor limiting the bandwidth of P-i-N photodetector is the RC charging time which comes from the change of storage charge in the junction. The parasitic components contributing to the RC time constant are series resistance in diode (R_S), load resistance (R_L), parasitic pad capacitance (C_p), and junction capacitance (C_j), as shown below:

$$f_{3dB,RC} = \frac{1}{2\pi\tau_{RC}} \ , \ \tau_{RC} = (R_S + R_L)(C_P + C_j) \ , \ C_j = \frac{\epsilon_s A}{T_{intrinsic}}$$

- $T_{intrinsic}$: intrinsic layer thickness
- ϵ_s: dielectric constant for material
- A: aperture area of device

Figure 6 shows the simulation based on the expression above with bandwidth ranging from 10 GHz to 50 GHz with different aperture sizes and thickness of the intrinsic layer. Assuming R_L = 50 Ω and C_p = 25 fF, we can see that in order to increase the bandwidth, we can either shrink the

aperture size or increase the thickness of intrinsic layer, which reduces the RC time constant. In order to get the total bandwidth of P-i-N photodetector, we need to consider the sum of both delays as shown below:

$$f_{3dB,total} = \left(\frac{1}{f_{3dB,RC}} + \frac{1}{f_{3dB,transit}} \right)^{-1}$$

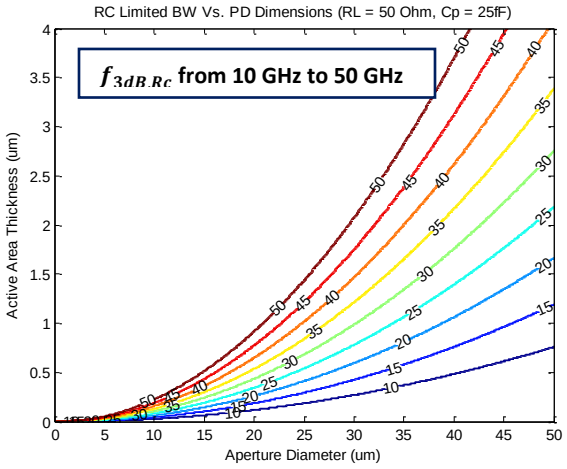

Figure 6: RC charging time limited bandwidth vs. different aperture diameters and thickness of intrinsic layer

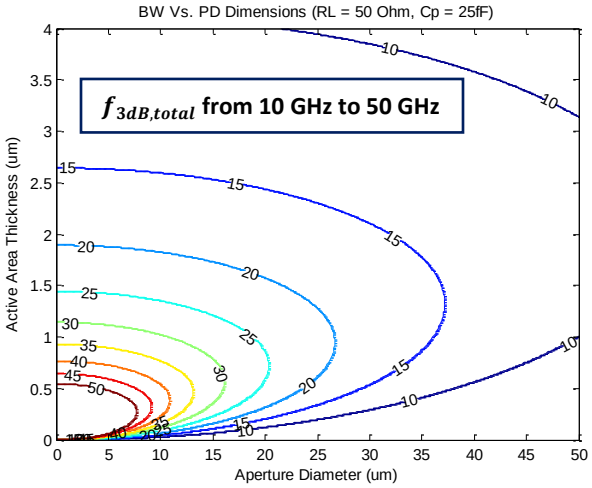

Figure 7: Total bandwidth vs. different aperture diameters and thickness of intrinsic layer [6]

Figure 7 shows the contours of total bandwidth from 10 GHz to 50 GHz. There is a trade-off in either continuing increase the aperture size or decrease the thickness of intrinsic layer. For our target value of 50 Gb/s data rate, the approximate bandwidth of 25 GHz needs to be achieved; therefore, our P-i-N photodetector has an optimal design of 0.75 μm in the thickness of intrinsic layer and 20 μm in the aperture size, as shown on the aqua contour in Fig. 7.

2. Characterization and modeling of P-i-N photodetector

After the fabrication is finished, we then perform surface illumination on the aperture indicated in Fig. 8 and measure the performance of the device. The measurement of the P-i-N photodetector includes measuring the output current from the photodetector as well as the frequency response, which are the two important measurements in photodetector characterization. Figure 9 shows the block diagram and setup for the measurement. We first measure the optical power from our VCSEL with a calibrated optical power meter, then couple the light from the VCSEL to our P-i-N photodetector with optical fibers and a lightwave probe. We then measure the output current from the photodetector and find the ratio of photocurrent to the available power from the VCSEL (with unit of A/W) to characterize the responsivity of P-i-N photodetector. We can use the same setup in bandwidth measurement with the aid of Keysight network analyzer and we can measure the 3dB bandwidth of our P-i-N photodetector. Figure 10 shows the microwave small signal model for the P-i-N photodetector for the bandwidth de-embedding and junction capacitance extraction. One-port s-parameter measurements are taken using a Keysight network analyzer using off-wafer calibration standards and on-wafer short-open de-embedding. The model is simulated using Keysight ADS and model parameters are adjusted to fit the measured s-parameters.

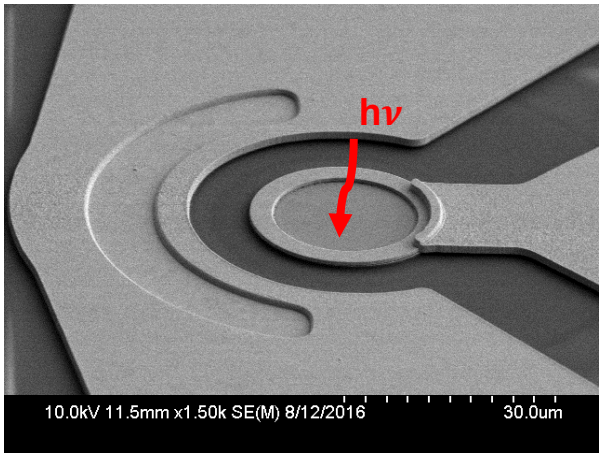

Figure 8: Top view of a 50 Gb/s P-i-N photodetector [6]

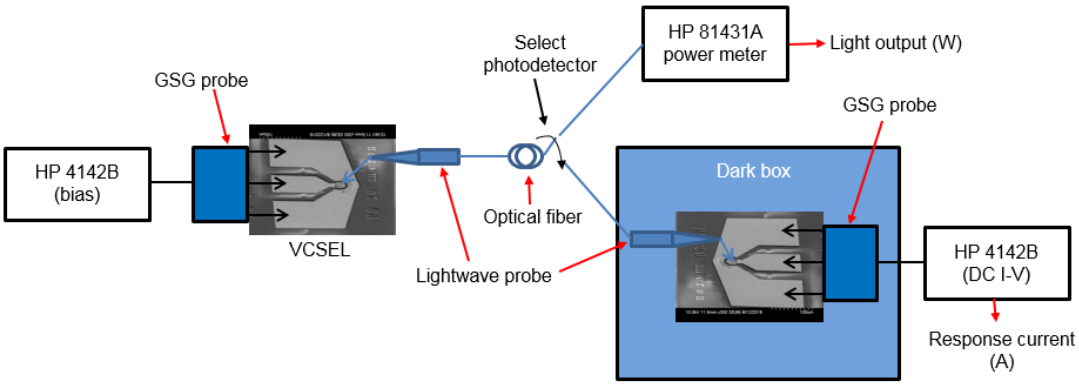

Figure 9: Responsivity measurement block diagram (top) and setup (bottom)

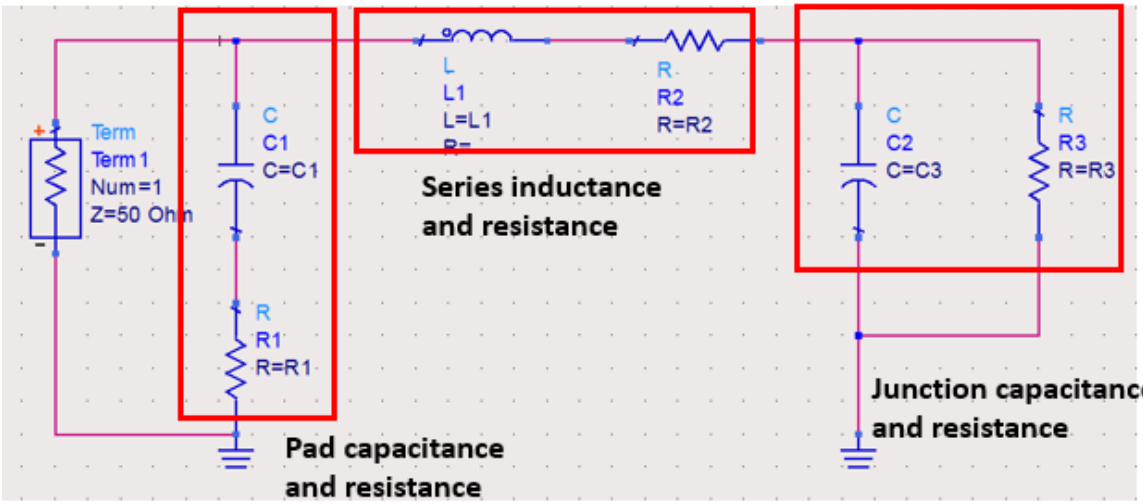

Figure. 10: Small-signal model of a P-i-N photodetector [6]

Fitted small signal model parameters of the P-i-N photodetector are given in Table 1 with different mesa diameters. In particular, we are interested in the capacitor C3 which represents the photodiode junction capacitance. A plot of fitted C3 against the junction area in Fig. 11 shows a linear dependence, as expected from a photodetector.

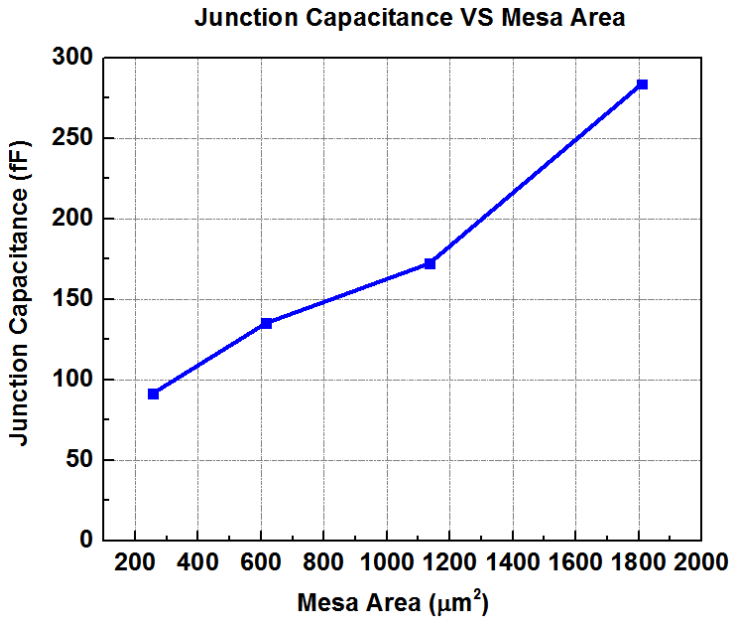

Figure. 11: Photodetector junction capacitance versus aperture area

Table. 1: Fitted small-signal model parameters of P-i-N photodetector with various mesa diameters

Diameter	C1 (fF)	C3 (fF)	L1 (pH)	R1 (Ω)	R2 (Ω)	R3 (kΩ)
48 μm	72.55	283.6	63.7	702.5	2.92	15.2
38 μm	71.29	170.05	74.63	666.26	2.46	14.55
28 μm	74.16	135.07	79.19	577.91	2.37	17.25
18 μm	18.66	91.29	80.69	506.5	2.34	14.51

After de-embedding the bandwidth of the P-i-N photodetector from the VCSEL, we can obtain the bandwidth of the photodetectors with various diameters shown in Fig. 12. The results indicate that in order to achieve higher bandwidth of the photodetector, we need to design smaller diameters to reduce the RC time constants.

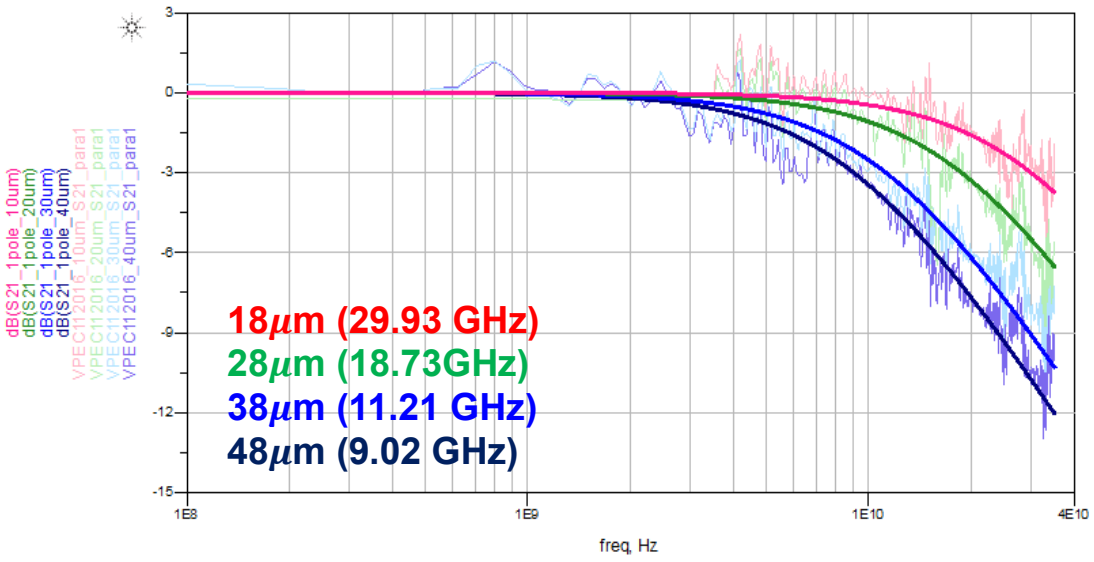

Figure. 12: Extracted bandwidth of the photodetectors after de-embedding

3. Conclusion and future work

The P-i-N photodetector has the advantages of easy fabrication and low noise, making it as great candidate to be used in the receiver of optical interconnects. With the high electrical field inside the intrinsic layer, photocurrent can be generated at the speed which is determined by transit time delay and RC charging time. In the development of P-i-N photodetectors, characterization through the microwave measurement and optical coupling is significant in order to help identify the optimal performance of the device and critical parameters for further improvement. However, from the results shown in this work, we know there is a trade-off between bandwidth and responsivity: if we want to achieve higher bandwidth (lower junction capacitance), we must design a photodetector with smaller aperture size; therefore, we will not have decent responsivity due to the small amount of light that is able to come into the aperture. In order to overcome this trade-off, it is necessary to put more effort into device structure improvement and re-design of layout.

References

1 J. E. Bowers and C. A. Burrus, “Ultrawide-band long-wavelength p-i-n photodetectors,” J. Lightwave Technol., vol. LT-5, pp. 1339–1350, 1987

2 Cisco Global Cloud Index, 2015-2020

3 C.H. Cox, Analog Optical Links: Theory and Practice, Cambridge University Press, 2006

4 G. Lucovsky, R. F. Scharz, and R. B. Emmons, “Transit-time considerations in p-i-n diodes,” J. Appl. Phys., vol. 35, pp. 622-628, 1964

5 J. E. Proesel, L. C. Schow, A. V. Rylyakov, “25 Gb/s 3.6 pJ/b and 15 Gb/s 1.37 pJ/b VCSEL-based optical links in 90nm CMOS,” ISSCC, 2012

6 A. Winoto, Y.-T. Peng, M. Feng, “Design and fabrication of high-speed PIN photodiodes for 50 Gb/s optical fiber links,” Compound Semiconductor Manufacturing Technology (CSMANTECH), 2017